EPJ manuscript No.
(will be inserted by the editor)

PIC simulations of ccrf discharges

P. Matthias[1], G. Bandelow[1], K. Matyash[1], J. Duras[3], P. Hacker[1], D. Kahnfeld[1], S.Kemnitz[2], L. Lewerentz[1] and K.F. Lüskow[1], J. Meichsner[1], and R. Schneider[1]

[1]Institute of Physics, Ernst-Moritz-Arndt-University Greifswald, D-17489 Greifswald, Germany
[2]Institute of Computer Science and Technology, University Rostock, D-18051 Rostock, Germany
[3]Nuremberg Institute of Technology, D-90489 Nuremberg, Germany

Received: date / Revised version: date

Abstract. Capacitively coupled discharges with a radio-frequency modulated voltage (ccrf) are important for plasma assisted material processing [1][2]. Experiments with electronegative oxygen ccrf discharges show a high-energy peak in the energy distribution of negative ions arriving at the anode, depending on the cathode material used. One possible explanation is ionization at or close to the surface of the cathode for the production of negative ions [3][4][5]. By introducing an additional surface ionization model into a Particle-In-Cell (PIC) simulation with Monte Carlo Collisions (MCC) [6][7] the experimental result is reproduced qualitatively. Comparison of one dimensional and two dimensional simulation results allows an improved understanding of the microscopic processes determining the dynamics of negative ions.

PACS. 52.40.Hf Plasma-material interaction, boundary layer effects – 52.40.Kh Plasma sheaths – 52.30.-q Plasma dynamics – 82.33.Xj Plasma reactions – 52.65.-y Plasma simulation

Motivation

In industrial applications plasma is used for plasma etching, thin-film deposition [8] and sputter techniques [1]. Especially reactive electronegative plasmas increase sputtering and deposition rates and are widely used in technology. For the treatment of surfaces it is important to know the detailed energy distribution functions (EDF) of the impinging ions, and in case of electronegative plasmas the EDF of negative ions as well. Experiments show high energy peaks in the EDF for negative ions arriving at the grounded electrode in an asymmetric ccrf discharge with oxygen as the process gas, depending on the powered electrode material used. Therefore, surface effects may be important for the EDF of the negative ions. Investigating surface effects and their impact on the plasma is the aim of this work.

Surface effects and secondary ion emission

In addition to secondary electron emission [9] there also exists **s**econdary **i**on **e**mission (SIE). Theoretical studies of surface ionization are mostly devoted to the production of positive ions from incident atoms of thermal energy [4]. The degree of ionization can be derived by applying thermodynamics.

The ionization coefficient $\alpha^+(M^+)$ is given by

$$\alpha^+(X^+) = \frac{n^+}{n} = \frac{1-r^+}{1-r} \cdot \frac{w^+}{w} \exp\left(\frac{\bar{\Phi}^+ + e\sqrt{eF} - I(X)}{k_B T}\right), \quad (1)$$

where n^+ and n are the numbers of positive ions X^+ and neutrals X coming from a unit surface area per unit time, w^+/w is the statistical weight ratio of X^+ to X, r^+ and r are the internal reflection coefficients at the potential barrier on the emitter surface, $\bar{\Phi}^+$ is the average work function, T is the absolute temperature at the surface, F is the externally applied field and $I(X)$ is the initial energy of the impinging atoms.

Equation (1) can also be used for a surface which emits negative ions. A negatively biased surface like the powered electrode in an asymmetric ccrf discharge is assumed with an equilibrium condition

$$X + e^- \text{ (in the substrate metal)} \leftrightharpoons X^- \quad (2)$$

at the surface. The equation for the negative ionization coefficient is derived in analogy to equation (1)

$$\alpha^-(X^-) = \frac{n^-}{n} = \frac{1-r^-}{1-r} \cdot \frac{w^-}{w} \exp\left(\frac{-\bar{\Phi}^- - e\sqrt{eF} + A(X)}{k_B T}\right), \quad (3)$$

where $A(X)$ is the electron affinity of atom X, $\bar{\Phi}^-$ is the average effective work function for producing the negative ion X^- on the metal surface and the other parameters are in analogy to the case of positive ion emission. No detailed theoretical and experimental studies of reflection coefficients exist r for negative ions. Therefore, no cross-section data for such processes are available. For the simulations in this work an empirical production efficiency $\eta = n_-/n_+$ is introduced for positive ions hitting a surface. n_+ is the number of incoming positive ions and n_- the number of emitted negative ions.

To get a microscopic understanding of the underlying physics a ccrf oxygen discharge is simulated kinetically with PIC-MCC [6]. This is necessary, because mean free paths are of the same magnitude as the electrode gap and relaxation of the distribution functions to Maxwell distributions due to collisions does not occur. This means that fluid models are incomplete and kinetic models have to be applied.

PIC-MCC method

The discharge of the experiment is operated in cylindrical geometry. For the region close to the center of the discharge a one-dimensional approach is usually used neglecting transport processes in radial direction. This can be further improved using a two-dimensional simulation in radial and axial direction. Particle-in-Cell (PIC) with Monte-Carlo-Collisions (MCC) methods simulate the motion of pseudo-particles, representing a large number of real particles, in continuous phase space while macro quantities like density or potentials are computed on stationary mesh points [10]. The method follows the trajectories of charged particles in self-consistent electromagnetic (in this case electrostatic) fields computed on a fixed mesh. The macro-force is then calculated from the field equations. Macro forces are used to avoid the computer time consuming particle-particle interactions which scale quadratic with the particle number N^2. In contrast to this, the particle-mesh method just scales with $N \log N$ and is hence much faster [6]. For the system studied here, neutrals are considered as a constant background due to their much higher density compared with the charged species and the rather low ionization degree in such discharges. The neutrals act as a kind of reservoir. Therefore, the collision dynamics is only resolved for the charged species. Here the same collision and cross sections were used as in [11].

Simulation of ccrf oxygen discharges

As standard parameters a pressure of 10 Pa and a peak-to-peak voltage of 800 V_{pp} are chosen. Pressure is reduced down to 2 Pa. The radio-frequency is set to 13.56 MHz as in experiment. PIC simulations work with normalized units to resolve the spatial (Debye length) and temporal (plasma frequency) properties. Reference parameters for the normalized PIC units are an electron density of $n_e = 5 \cdot 10^9\,/\mathrm{cm}^{-3}$ and an electron temperature of $T_e = 4\,\mathrm{eV}$. This results in a Debye-length of the system of $\lambda_{Db} \approx 0.021$ cm and an electron plasma frequency of $\omega_{pe} \approx 3.99 \cdot 10^9\,\mathrm{s}^{-1}$. The electrode gap of the experiment is 5 cm. Studies have shown that the choice of η in a short range of [0.01...0.1] has only little influence on the plasma. In the following simulations only secondary negative ion emission is added for the powered electrode as an additional wall process with an efficiency of $\eta = 0.03$ [9] to separate the influence of other processes.

Discharges with secondary ion emission

Including the SIE injection model of oxygen anions at the powered electrode, one can see in figure (1) that the number density of the anions is slightly shifted towards the powered electrode compared with the grounded electrode where no SIE model is applied.

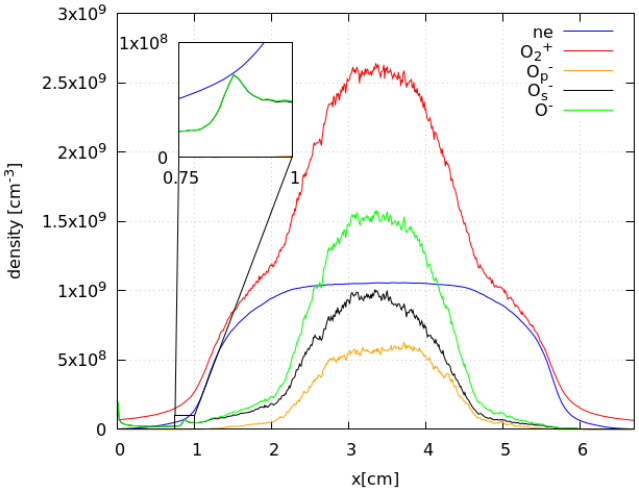

Fig. 1: Densities of e^-, O_2^+ and O^- with secondary ion emission at the powered electrode (η=0.03). The pressure was 5 Pa and the rf voltage was set to $U_{rf} = 800\,V_{pp}$. The zoomed in area shows the small density peak of O_s^- at the powered electrode sheath edge. The powered electrode is located at x=0 cm.

The anion number densities were separated into the ones produced by volume processes in the plasma O_p^- and the ones produced at the surface O_s^-.

A small density peak of O_s^- at the sheath edge in front of the powered electrode is noticeable. It forms due to elastic collisions of the anions O_s^- in the sheath.

The O_s^- get accelerated in the sheath, cross the bulk and then get reflected in the sheath of the grounded electrode similar to the movement of the electrons, but on a larger time scale (microseconds for electrons but milliseconds for negative ions).

In the energy distributions of O_s^- an additional high-

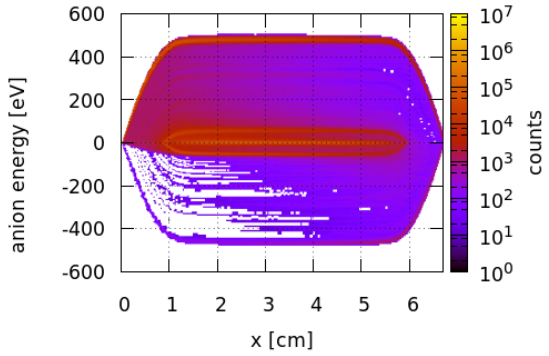

Fig. 2: Energy distribution function of O_s at 5 Pa and a driver voltage of 800 V_{pp}. The "sign" of the energy indicates the direction of the particles. The powered electrode with additional SIE is located at x=0 cm.

energy peak builds up (figure (2)). It decays with the time of flight (distance to the powered electrode) due to charge-exchange and elastic collisions with neutral molecules O_2 which results in an energy loss for the anions. Also, a part of the anions get detached by neutrals or recombine with positive ions. In existing publications it is assumed that if an anion collides with a neutral it is very likely to get detached due to the cross-section [12].

In figure (3) the difference between the numbers of elastic collisions for a normal discharge and a discharge with additional SIE are shown. It is obvious that the anions undergo elastic collisions which leads to an energy loss and a continuous plateau in the energy distribution. Most elastic collisions occur in the bulk while the sheaths are mostly collisionless. But for the surface ions O_s^- one can see that the collisions in the powered electrode sheath cannot be neglected. They lead to an energy loss for the anions which influence their energy distribution.

In figure (2) a structure in the lower energy region in the bulk can be seen. The elastic collisions produce a peak structure in the ion energy distribution. To study the sheath dynamics during a rf period one phase of the energy distribution function for O_s^- is shown in figure (4). The density peak at the sheath edge (as seen earlier in figure (1)) originates from the low-energy peak in the energy distribution. With the average ion energy in the sheath and the rf-cycle time τ_{rf} one can calculate the transit time τ_{ion}. Assuming an average ion energy of $40 - 50$ eV and a traveled distance of $\approx$1 cm it follows the ratio $\frac{\tau_{ion}}{\tau_{rf}} \approx 4.5$. This is the number of rf-cycles an anion stays in the

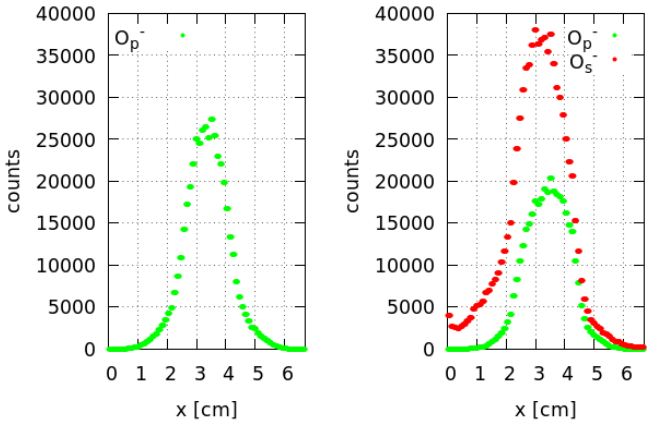

Fig. 3: Number of elastic collisions of negative ions O^- with neutral molecules O_2 per 10^5 time steps without SIE (left) and with SIE ($\eta = 0.03$) (right) where the two O^- species are separated. The powered electrode is located at x=0 cm

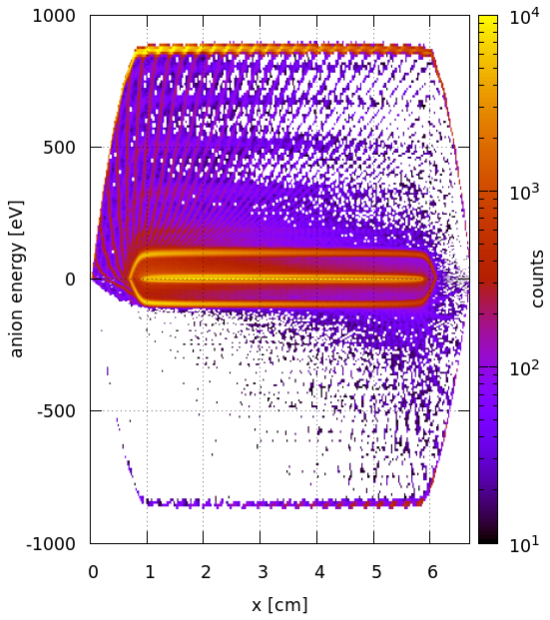

Fig. 4: Same energy distribution as in figure (2) with an applied driver voltage of 1600 V_{pp} at t=0 of the rf cycle , which is equal to a voltage of U(t)=0 at the powered electrode.

sheath. Hence the number of peaks in the negative ion energy distribution must be similar. In figure (4) one can see that 4-5 low energy peaks in the sheath build up through elastic collisions of the negative ions with neutrals. At the sheath edge these energy density cycles overlay. Additional simulations have shown that without elastic collisions no additional density peak builds up. Hence, the energy plateau of the anions is mainly influenced by elastic collisions. The spatial resolved IEDF leads directly to the density distribution of the negative ions O_s^-. The density peak at the sheath edge (see figure (1)) originates from the low-energy peak in the energy distribution of the negative surface ions O_s^-.

In the experiment the powered electrode potential is shifted by the self-bias voltage due to the asymmetry of the electrodes resulting in an asymmetric potential. As a consequence of this asymmetry the anions can get enough energy to get to the grounded electrode while in the 1d3v simulation they get reflected by the sheath potential due to its intrinsic symmetry. This results in a higher probability of elastic collisions with neutrals since the ions stay longer in the discharge leading to to the discussed density peaks at the sheath. Figure (5) confirms that negative ions produced at the surface may lead to the measured high-energy peak. Since the experiment is driven by an adjustable network power, while the simulation depends on the voltage at the powered electrode, the results are only comparable on a qualitative level. But the energy distribution function of the simulation has additional low energy peaks (at $< 100\,\mathrm{eV}$), too. They are probably created due to the intrinsic symmetry in the 1d3v simulation. In the experiment all high-energy anions are detected and thereby removed from the discharge.

Additional studies have been done varying pressure, voltage and injection coefficient. Their results support the hypothesis that the high energy peaks are created by secondary ion emission.

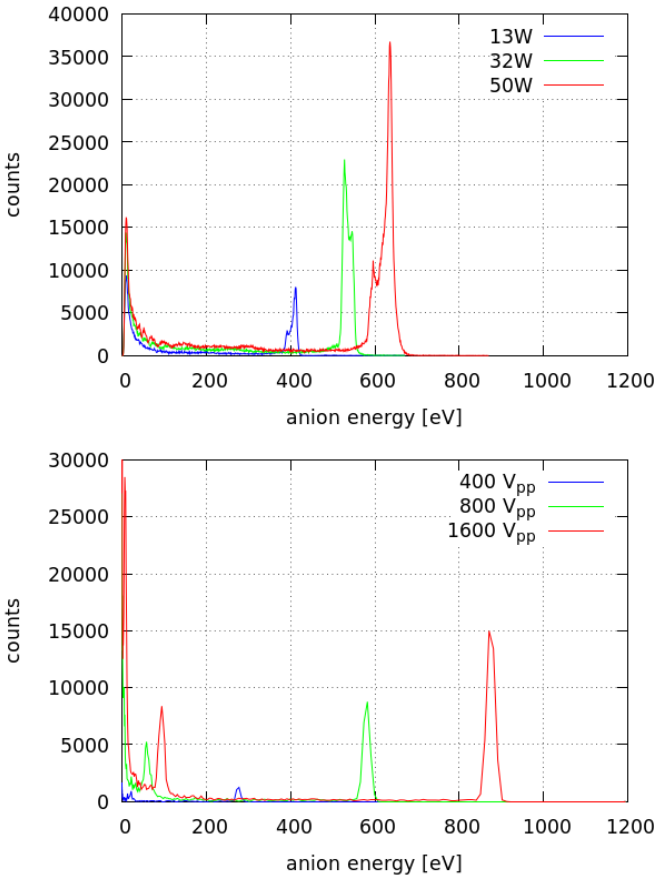

Fig. 5: Energy distribution of negative ions O^-. Top: Experimental results for MgO measured at the grounded electrode for different rf powers. Bottom: Simulation result with 1d3v PIC simulation with additional SIE, taken at the grounded electrode sheath edge 6 cm at different rf powers at 5 Pa and $\eta = 0.03$.

Two-Dimensional PIC simulations

To be able to study also the effect of self-bias a two-dimensional r-z PIC code is used to simulate a capacitively coupled rf discharge.

To realize an asymmetric discharge the size of the powered electrode is set smaller than the size of the grounded electrode. In an asymmetric discharge the high mobility of the electrons charges the powered electrode, which then gets a negative self-bias voltage. The self-bias voltage is implemented using experimental values as an dc-offset of the rf-voltage at the powered electrode. This approach fulfills the flux balances [13] self-consistently.

To realize the parameters of the experiment, which uses electrode radii of a few centimeters. A powered electrode with a radius of 1.5 cm and an grounded electrode with a radius of 4.5 cm is used in the model and a grounded box is put around it. The electrode gap is about 2.5 cm. Due to the asymmetric distributions of the total currents to the walls and electrodes a negative self-bias voltage at the powered electrode according to the experimental values is added.

In figure (6) the negative ion number density is shown for pressures of 10 Pa and 6 Pa with an applied rf voltage of 800 $\mathrm{V_{pp}}$. One can see that the bulk region is deformed at the powered electrode side due to the self-bias voltage of 200 $\mathrm{V_{sb}}$ leading to a reduced electron flux towards the powered electrode.

There is a higher flux of positive ions towards the powered electrode than to the grounded electrode due to the self-bias voltage. In ~~a~~ this one-dimensional simulation the total ion flux towards the powered electrode and the powered electrode sheath width are underestimated, because no self-bias can exist. There are other approaches like voltage waveform tailoring [14][15] or spherical 1d codes [16] to simulate self-bias voltages, but here we stick to a mono frequency approach. Still, the form of the number density distributions is nearly the same, which shows that a one-dimensional simulation is a good approximation near the center.

A special interest exists to study the energy distributions,

especially of the negative ions, while applying the former model of SIE. Following the argumentation of the one-dimensional model the injected anions should not be able to stay in the discharge, due to the additional energy from the self-bias voltage (s. figure (7)).

The secondary negative ions, which do not collide or

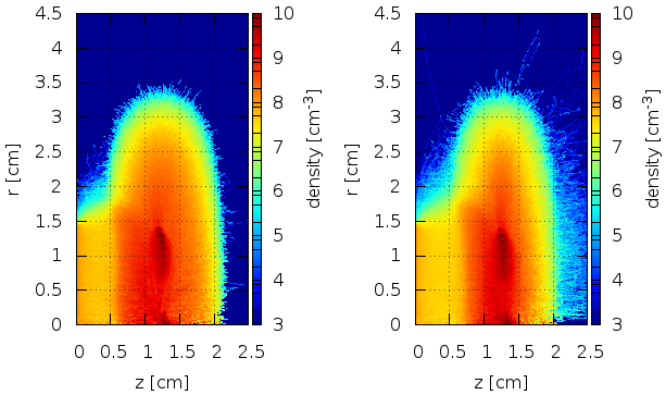

Fig. 6: Negative ion density distribution at 10 Pa (left) and 6 Pa (right). The powered electrode is located at z=0 cm.

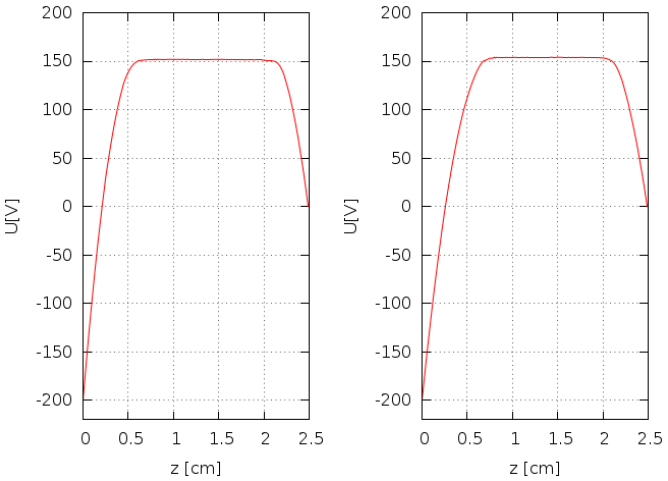

Fig. 7: Averaged Potential with self-bias voltage at the powered electrode shown along the axis at 10 Pa (left) and 6 Pa (right). The powered electrode is located at z=0 cm.

get detached in the bulk, obtain enough energy from the self-bias voltage to cross the grounded electrode sheath and impinge on the grounded electrode. This explains the discrepancy in the one-dimensional model, which is lacking this physics and is therefore not able to reproduce the experiment.

Calculating the negative ion EDF at the grounded electrode, one can compare the results with the experiment. In figure (8) the same high energetic peak shows up as in the experiment. This supports the idea that the observed high energetic peaks in the EDF of the negative ions at

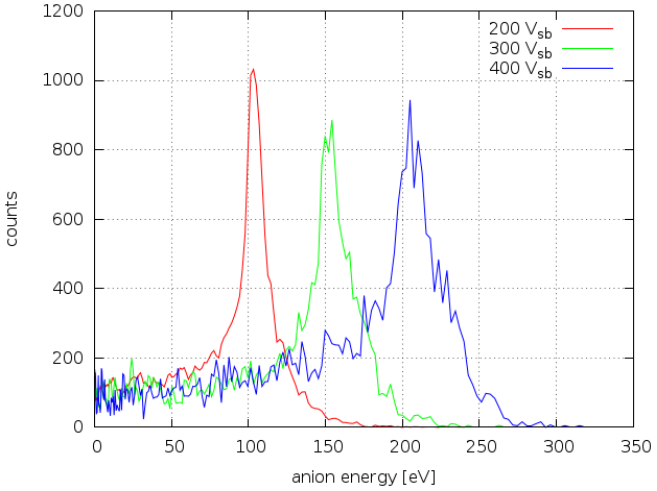

Fig. 8: Negative ion velocity distribution at the grounded electrode at 4 Pa and 800 V_{pp} with different self-bias voltages.

the grounded electrode are produced by surface effects at the powered powered electrode.

Summary

In this work 1D and 2D PIC-MCC models were used to simulate electronegative ccrf discharges with oxygen as process gas. The 1D simulations demonstrate the importance of elastic collisions for surface anions which leads to an energy loss and a continuous plateau in the energy distribution function. However, the 1D model lacks the possibility to study the influence of self-bias. Therefore, 2D simulations were done including the experimental self-bias and geometrical asymmetries. The results support the hypothesis that the high energy peak in the measured energy distribution function of negative ions at the grounded electrode originates from secondary negative ions created at the surface.

In the future the 2D PIC simulation can be used to study further aspects of asymmetric electronegative discharges, e.g. introducing complex sputter models. This will also allow to apply it to industrial applications like etching for a more detailed microscopic description.

Literature

[1] M. Zeuner et al. “Sputter process diagnostics by negative ions”. In: *Journal of Applied Physics* 83.10 (1998), pp. 5083–5086.

[2] J. T. Gudmundsson and Bruno Ventéjou. “The pressure dependence of the discharge properties in a capacitively coupled oxygen discharge”. In: *Journal of Applied Physics* 118.15 (2015), p. 153302. DOI: 10.1063/1.4933293.

[3] E. Stoffels, W. W. Stoffels, and G. M. W. Kroesen. "Plasma chemistry and surface processes of negative ions". In: *Plasma Sources Sci. Technol.* 10 (2001), pp. 311–317.
[4] H. Kawano and F. M. Page. "Experimental methods and techniques for negative-ion production ionization". In: *International Journal of Mass Spectrometry and Ion Physics* 50 (1983), pp. 1–33.
[5] Ihor Korolov et al. "The influence of electron reflection/sticking coefficients at the electrodes on plasma parameters in particle-in-cell simulations of capacitive radio-frequency plasmas". In: 25 (Jan. 2016), p. 015024.
[6] D. Tskhakaya et al. "The Particle-In-Cell Method". In: *Contrib. Plasma Phys.* 47.8-9 (2007), pp. 563–594.
[7] J T Gudmundsson, E Kawamura, and M A Lieberman. "A benchmark study of a capacitively coupled oxygen discharge of the oopd1 particle-in-cell Monte Carlo code". In: *Plasma Sources Science and Technology* 22.3 (2013), p. 035011.
[8] U. Cvelbar, M. Mozetic, and M. Klansjek-Gunde. "Selective oxygen plasma etchin of coatings". In: *Plasma Science, IEEE* 3.2 (2005), pp. 236–237.
[9] J. Meichsner et al. "Nonthermal Plasma Chemistry and Physics". In: (2013).
[10] K. Matyash et al. "Particle in Cell Simulation of Low Temperature Laboratory Plasmas". In: *Contrib. Plasma Phys.* 47.8-9 (2007), pp. 595–634.
[11] F.X. Bronold et al. "Radio-frequency discharges in oxygen: I. Particle-based modelling". In: *J. Phys. D: Appl. Phys.* 40 (2007), pp. 6583–6592.
[12] C. Küllig., J. Meichsner, and K. Dittmann. "Detachment-induced electron production in the early afterglow of pulsed cc-rf oxygen plasmas". In: *Physics of Plasmas* 19 (2012), pp. 73–100.
[13] Z. Donkó et al. "PIC simulations of the separate control of ion flux and energy in CCRF discharges via the electrical asymmetry effect". In: 42 (Jan. 2009), pp. 25205–10.
[14] E. Schüngel et al. "Tailored voltage waveform capacitively coupled plasmas in electronegative gases: frequency dependence of asymmetry effects". In: *Journal of Physics D: Applied Physics* 49.26 (2016), p. 265203.
[15] Aranka Derzsi et al. "Experimental and simulation study of a capacitively coupled oxygen discharge driven by tailored voltage waveforms". In: 25 (Feb. 2016), p. 015004.
[16] M. A. Liebermann and A. J. Lichtenberg. "Principles of Plasma Discharges and Materials Processing". In: (2005).

Support from the Deutsche Forschungsgemeinschaft through Project No. B5 and No. B10 of the Transregional Collaborative Research Center SFB/TRR 24 is greatly acknowledged. The experimental measurements were performed by JM. The code was developed by KM and further designed by RS, PM, SK, KFL, DK, JD and GB. All authors contributed to the conceptual design of the work, participated in the discussion of the results, provided valuable comments, and contributed to the revision of the manuscript.